

# An Examination of the Validity of MRPS Method for the Detection of Label-free *E. Coli* and Enterococci in Ships Ballast Water

M M Maw<sup>1</sup>, J S Wang<sup>2,\*</sup>, K Z Yu<sup>1</sup>, Y J Wang<sup>2</sup>, B W Dai<sup>2</sup>, X D Wu<sup>3</sup> and X X Pan<sup>1,\*</sup>

1 College of Marine Engineering, Dalian Maritime University, Dalian, 116026, China

2 College of Information and Science Technology, Dalian Maritime University, Dalian, 116026, China

3 Jiangsu Jimbio Technology Co., Ltd, Changzhou, 213022, China

Email: wangjsh@dlmu.edu.cn

**Abstract.** To test for compliance with the D-2 standard for ballast water management convention of the International Maritime Organization, the bacteriological quality of ship's ballast water is determined to evaluate the risk of invasion of non-indigenous species both onboard ship and in Port. In this article, hydrodynamic flow focusing particles viewed through a microfluidic resistive pulse sensor (MRPS) was used to detect the pathogenic bacteria from ship's ballast water. *Escherichia coli* and *Enterococci* were addressed as bacterial indicators to determine of their characteristic and concentration. The system provided the individual particle-by-particle readout in rather large 20  $\mu\text{m}$  x 10  $\mu\text{m}$  x 8  $\mu\text{m}$  (length x width x height) horizontal rectangular microchannel duct. The average volume flow rate was 4.5  $\mu\text{l}/\text{min}$ . However, it returned online and real time results for a complete of 30  $\mu\text{l}$  sample volume during 15 min. The system was low maintenance, high in sensitivity, good accuracy and reliable. Targeted bacteria needed neither labelling nor extracting DNA.

## 1. Introduction

An estimated over 7,000 marine species are transmitted daily with ship's ballast water to new environments [1]. A few non-indigenous species have already had irreversible impact on human health, ecosystems or economies [2]. Regarding the negative impact of organisms by ship's ballast water discharge into a new environment, the International Maritime Organization (IMO) adopted the "International Convention on the Management of Ships Ballast Water and Sediments" (hereafter it will be used as the convention). In the convention, ships need to manage their ballast water to avoid the uptake or discharge of harmful aquatic organisms and pathogens in ballast water and sediments [3]. Since the convention entered into force on 8 Sept, 2017 [4], all ships need to comply with the D-2 Standard of convention. The convention limited the concentration of indicator microbes for *Escherichia coli* (*E.coli*), *Enterococci* and toxicogenic *vibrio cholera* [5]. The quality of ship's ballast water will be accessed before discharging and it becomes a technical challenge.

The most well-known methods of detection for indicative microorganisms sample from ships ballast water are Adenosine triphosphate (ATP) [6-8], Fluorescein diacetate staining (FDA) [8-10], pulse amplitude-modulation (PAM) fluorometry [8,9,11,12], Flow cytometry [8,9,13,14] and Polymerase chain reaction (PCR) [15,16]. However these conventional methods for monitoring and analysis on bacteria are bulky, labour intensive, time consuming and depend on the land based laboratory. The



development methods and portable devices that can rapidly on-line detection and real-time determine the number of seaborne single microorganisms will become necessary.

In the recent era, the advantageous features of microfluidics technologies can characterize the mechanical, electrical and biophysical properties at individual cell level [17-19]. Microfluidic individual cell analysis systems provide for counting, trapping, focusing, separating, sorting, characterization and identification. Many researchers invented and reported microfluidic based analysis tools for single cells by combining the conventional methods of ATP [20, 21], PCR [22, 23], fluorescent in-situ hybridization (FISH) [24,25] and surface enhanced Raman scattering (SERS) [26,27]. Some of their techniques can detect single cell with high accuracy. Nevertheless, the detection can be performed by sophisticated and specialized equipment. Also some techniques need fluorescent activated cell sorting, extraction DNA, and staining bacteria etc. which are done in the laboratory. Among these detection systems, the Coulter counting principle is simple for counting cells [28] in the electrolytic fluid, generally count cells from blood. Debloris and Bean [29] first demonstrated the use of submicron resistive pulse sensor (RPS) which based on Coulter principle for the detection and characterization of nanoscaled objects, including nanoparticles and viruses. The resistive pulse sensing with the demonstration of single stranded DNA detection using a biological pore was introduced by Kasianowicz et al [30]. Due to RPS's sufficient sensitivity simplicity and cost-effectiveness, it has been increasingly applied in bio-sensing. To date, numerous RPS are advanced with synthetic biological pore and microfluidic sensors by many researchers [31-33]. Lab-on-a-chip with resistive pulse sensors have been used for some time and can be applied via a laser or fluorescent light to detect chlorophyll of microalgae from ship's ballast water [34-36].

To extend our experiments in detecting and analysing system which already successful detected of microalgae [37, 38] in the few years ago, now we addressed bacteriological organism detection in this article. Label-free *Escherichia coli* (*E.coli*) and *Enterococcus faecalis* (hereafter named *Enterococci*) were applied as the indicator samples. They are described as indicator microbes in IMO D-2 standard. A combination of microfluidic sample handling chip design and the phenomena of microscale hydrodynamic flow has been used to improve the detecting sensitivity in this paper.

## 2. Materials and methods

### 2.1. Sample bacteria preparation

The strains of *Escherichia coli* (*E.coli*) (ATCC 25922) and *Enterococcus faecalis* (ATCC 29212) were used in our experiments. They were provided by Jie Su et al., Marine Ecology Department, National Marine Environmental Monitoring Centre (Dalian, China). Cultured bacteria were added in the natural marine water from Dalian sea which was taken by sterile flask submerged to 1m below the water surface. The average dimensions of *E.coli* are 0.5  $\mu\text{m}$  ~ 0.78  $\mu\text{m}$  diameter & 1  $\mu\text{m}$  ~ 2  $\mu\text{m}$  length, and *Enterococci* are 0.45  $\mu\text{m}$  ~ 0.65  $\mu\text{m}$  diameter & 1  $\mu\text{m}$  ~ 1.5 $\mu\text{m}$  length.

### 2.2. Design of microfluidic chip

A microfluidic chip is the detection platform of the MRPS and the detail design of detecting zone is shown in Figure 1. It was composed of a sample well, a sheath well, a right sensing well, a left sensing well, a main waste well, a complementary waste well, two sheath channels, two detecting channels, a nozzle jet design main microchannel and a detecting zone or sensing gate. The microfluidic chip was mainly made by polydimethylsiloxane (PDMS) (Sylgard 184, Dow Corning, Midland, MI, USA) with the general rectangular size of 40 mm long, 18 mm wide and 3.5 mm thick. The main channel was started from the right quadrants of sample well and it was gradually tapered from 800  $\mu\text{m}$  wide to 400  $\mu\text{m}$  for 6.5 mm long and again suddenly tapered down to 200  $\mu\text{m}$  for 1 mm long to get hydrodynamic focusing particles at detection zone and to avoid the back pressure on the particles in the channel. The width of sheath channels was 200  $\mu\text{m}$  with elliptical shape ways for 13 mm long from the centre of sheath well. The detecting channels width was 100  $\mu\text{m}$  for the first half part and 200  $\mu\text{m}$  for the second half with 45 degrees inclined to the main channel and 6 mm long from centre of sensing well to the main channel. The height of all channels was 8  $\mu\text{m}$ . The channel to complementary waste well was a branch from main channel with 45 degree inclination. All wells were punched the holes with 3.5mm

inner diameter on the PDMS. The detection zone was situated at the center between sample well and main waste well. It is a rectangular shape with 20  $\mu\text{m}$  length, 10  $\mu\text{m}$  width and 8  $\mu\text{m}$  height. The fabricated PDMS solid was bounded on a glass substrate which has 50 mm long, 24 mm wide and 1.07 mm thick (CITOGlas, Suzhou, China) by plasma cleaner.

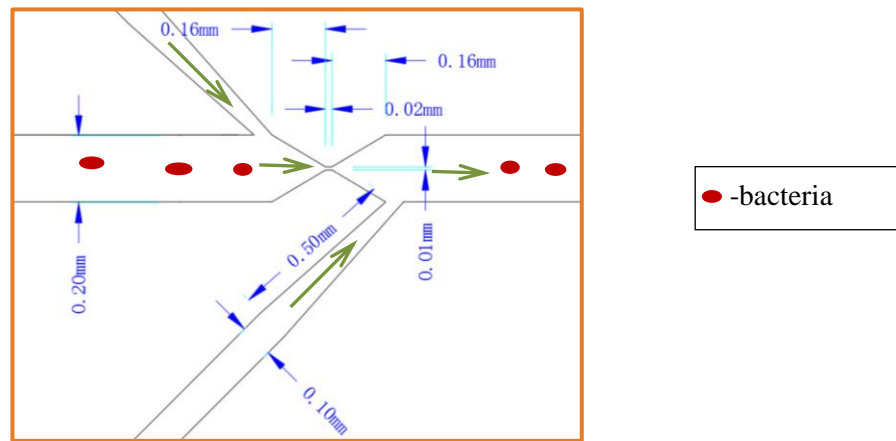


**Figure 1.** Structural design of detecting zone on a hydrodynamic focusing microfluidic chip.

### 2.3. Design and working principle of MRPS detection systems

The detecting system was mainly composed of a base unit, power supply unit, signal detection unit, signal processing unit, data acquisition unit and display unit. The principle of MRPS detection system is as shown in Figure 2. The base unit is included a PDMS microfluidic chip and four electrodes. In the power supply unit, the regulated DC power supply (HY1712-2S 0-50V 0-2A, Suzhou, China) was fixed at 24V and the positive charged was connected to the platinum electrode which embedded in the sample well while the negative end was connecting with the silver electrode of the main waste well. In the signal detection unit, the detecting circuit was connected to the electrodes of left and right sensing wells to receive the increase resistance as different potential voltages whenever the bacteria cells or particles were passing at the sensing gate. Data acquisition equipment NI USB-6259 DAQ board (National Instruments, Austin, TX, USA) was used to collect the results output signals from signal processing unit. In the display unit, LabVIEW software (2011 version, National Instruments, Austin, TX, USA) in personal computer received the data from DAQ board and finally displayed the real-time signal pulse results on the screen.

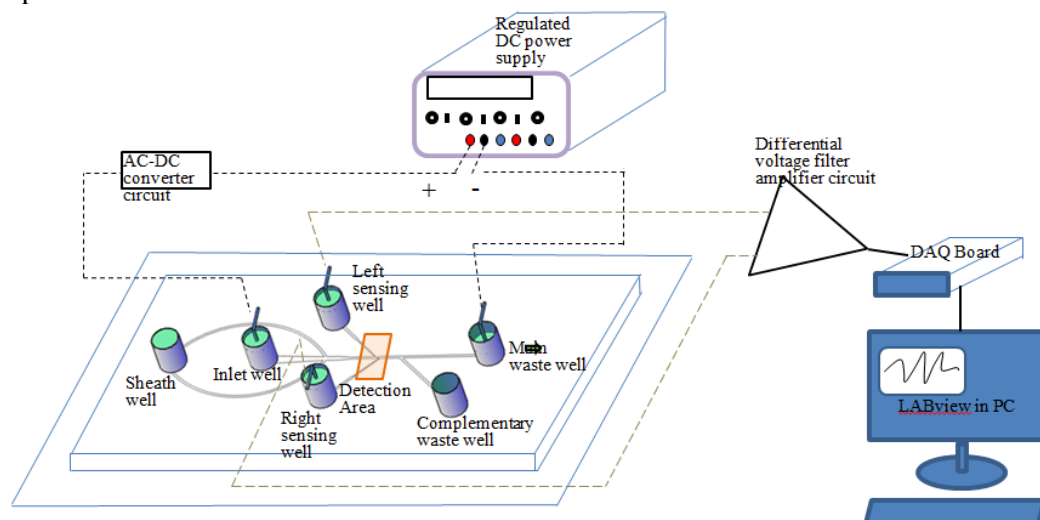


**Figure 2.** The principle diagram of MRPS detection system.

First of all, the microfluidic chip was placed in the base unit and four electrodes were embedded into the corresponding wells. Secondly the 30  $\mu\text{l}$  volume of sample solution was loaded into the sample

well. Then the left and right sensing wells were filled with 30 $\mu$ l phosphorous buffer solution (PBS) while the sheath well was fully added with 35 $\mu$ l of PBS. After that, the main waste well was filled with 10 $\mu$ l of PBS but complementary waste well was intentionally empty. The diffusion of the sample solution in the channels can be seen clearly by naked eyes. At the same time the power was supplied to the whole system as the third step.

When the power supply is applied, the main channel can be equivalent to three resistors connected in series. The main channel section of the sample well to the left end of the detection zone can be equivalent to one resistance ( $R_1$ ), the detection zone can be equivalent to one resistance ( $R_2$ ), and the main channel segment of the waste well can be equivalent to one resistance ( $R_3$ ).

When a cell or particle is aspirated through the detection area, it is replaced in the solution and it blocks the electric field. Then the resulted resistance in the detection area is significantly changed. The total change of resistance at the detection zone is achieved as the change of voltage at two ends detection channels by our system design. The value of total voltage changes can be calculated with the equation (1) [39, 40].

$$\Delta V_{output} = -A \frac{(R_1 + R_3) \Delta R}{(R_1 + R_2 + R_3)^2 + (R_1 + R_2 + R_3) \Delta R} V \quad (1)$$

where  $\Delta V_{output}$  is the potential difference between two ends of the detection zone due to increasing resistance by sample,  $V$  is the voltage difference between the sample well and the waste well,  $\Delta R$  is increased resistance by targeted sample when passing through the detection zone,  $A$  is the voltage gain by amplifiers

All targeted samples are carried out for detection at the detection zone under real time situation. Data acquisition unit collects the results from the signal processing unit. Finally all detected RPS signal amplitudes are displayed on display unit which is a PC with LabVIEW software. Every test has been repeated 3 times to get the system accuracy.

#### 2.4. Application of Maxwell's approximation theory

According to the Coulter counter theory by DeBlois and Bean [29], the resistance ( $R$ ) of a rectangular detecting channel is,

$$R = \frac{\rho L}{A} \quad (2)$$

where  $\rho$  is the resistivity of electrolyte fluid,  $L$  is the length of the detecting channel,  $A$  is the cross sectional area of rectangular detecting channel

When the detecting channel is filled with a small particle, the resistance will be changed. The expected resistance of a rectangular detecting channel containing a particle is,

$$R_{exp} = \frac{(\rho_{exp})L}{A} \quad (3)$$

By Maxwell's approximation theory for an insulating particle [41, 42], the value of  $\rho_{exp}$  becomes:

$$\rho_{exp} \approx \rho \left( 1 + \frac{3}{2} v_f \right) \quad (4)$$

where  $v_f$  is the ratio of particle volume to detecting channel volume;  $d$ ,  $l$  and  $r$  are diameter, the length and the radius of particle

Therefore, the increased resistance ( $\Delta R$ ) by particle in the detection channel is achieved by subtracting from expected resistance containing particle to the channel resistance without particle.

$$\Delta R = R_{exp} - R = \left( \frac{3}{2} v_f \right) R \quad (5)$$

According to equations (1) and (5), the amplitude of RPS output in voltage unit can be carried out.

### 3. Results and discussions

#### 3.1. Effectiveness design results of MRPS system

The detection sensitivity of resistive pulse signal depends on the design and fabrication of the microfluidic chip. It means the chip has a direct impact on the results of the experiments. Its characteristics will result in poor bacteria mobility.

The cross sectional area of sensing zone should be compared with the sample particle size to ensure that the particles can move individually in the microchannel. Both theoretically and practically, the wider area may allow flow particles to overlap. The risk of channel clogging increases with smaller area as well as the back pressure. The physical dimensions of the main channel are much larger than the detecting cross sectional area. This use of hydrodynamic focusing prevents channel blocking.

Moreover hydrodynamic focusing through sheath flows will provide the individual particle to centre position within the flow. Also sheath flows from two channels are kept at uniform velocity and constant pressure by providing one central sheath well. This will align the cells or particles into the narrow stream within a wider channel. The weaknesses of using sheath flow are sample dilution and faster levelling between samples well and waste well. To overcome this issue, a complementary waste well is addressed on our system design with intentionally empty fluid at the beginning of experiment. The flow velocity can be controlled by levelling of all wells simultaneously. Our system allows adding PBS buffer solution while operating the system at the sheath well and two sensing wells. And it also allows taking out the waste solution from the waste well and the complementary waste well without influencing to the experiment results. This way the experiment can be continued detecting sample bacteria until it has finished the sample well. By meeting the fluids from sheath channels and from the sample well at the main channel, an aggregation effect appeared which can prevent the blocking and can avoid the sample bacteria attaching at the wall. PBS solution also helped the bacteria from aggregation in the main channel. Furthermore, embedded sensing electrodes at opposite sides (left and right) provided a homogenous electric field, which is more tolerant to the position of the particle in the main microchannel. The time for the whole experiment depends on sample volume size, sample concentration and sample flow rate. Generally we finished one complete experiment in 15 min for 30  $\mu\text{l}$  sample size with 4.5  $\mu\text{l}/\text{min}$  volume flow rate. In addition to, the passage length dimension of sensing gate was determined two times the width to obviate much noise resistance rather than signal peak. This selection got the high signal-to-noise ratio in the detection system.

### 3.2. Examining the validity of MRPS detection system

To check the validity of the MRPS detecting system, we considered the standard curve for the relationship between sizes of particles, their volumes and amplitudes of RPS output voltage. Five sample of polystyrene particles such as with the diameter of 0.5  $\mu\text{m}$ , 0.6  $\mu\text{m}$ , 0.9  $\mu\text{m}$ , 1  $\mu\text{m}$  and 2  $\mu\text{m}$  were chosen for detection experiments due to the detection allowance percentage of the cross sectional area of the detecting duct. Specific sample particles were spiked separately in PBS solution tube. At first, 0.9  $\mu\text{m}$  particles were pipetted into the sample well and recorded the RPS signal peaks and detail information in excel data sheets with the aid of LabVIEW software. Then 0.5  $\mu\text{m}$ , 0.6  $\mu\text{m}$ , 1  $\mu\text{m}$  and 2  $\mu\text{m}$  diameter particles were separately loaded into the sample well at different times and recorded the corresponding differential output voltages of all detected sample particles. The experiment results generally give the same height of amplitude of signal pulses for certain spherical shape but there was a range in results sometime due to the case of coincidence or faster speed. So, we calculated the average amplitude value for each sample particles size and based on 15 min duration detection. They are 0.328 V, 0.5364 V, 0.8875 V, 1.554 V and 10 V respectively for 0.5  $\mu\text{m}$ , 0.6  $\mu\text{m}$ , 0.9  $\mu\text{m}$ , 1  $\mu\text{m}$  and 2  $\mu\text{m}$  diameter particles. The volumes of each particle are easily calculated with the mathematical formula of sphere and they are 0.065476  $\mu\text{m}^3$ , 0.113143  $\mu\text{m}^3$ , 0.381857  $\mu\text{m}^3$ , 0.52381  $\mu\text{m}^3$  and 4.18879  $\mu\text{m}^3$  respectively. According to Coulter counting base RPS theory, the larger the volume of the particle, the larger the resistance and related differential voltage pulse will be large. The volume of particles is exponentially increasing depending on the size of particle as well as the amplitudes of voltage output which are exponentially increased. The theory was verified using our detection system with a graph demonstrating the relationship between signal pulses amplitude and volume and diameter of particles (see in Figure 3). In short summary, the amplitude of differential voltage output is linearly changed with the volume of particles (see in Figure 4) and this relation is expressed in equation as below.

$$y = 2.3418x + 0.1915 \quad (6)$$

where  $y$  = amplitude of increased RPS output voltage (V), and  $x$  = volume of particle ( $\mu\text{m}^3$ )



Both of the standard curve graph and linear relationship graph ensure the validity of detection system for real time detecting small individual particles with the maximum system error is lesser than 1%. Therefore, the detection system is reliable to do more experiments.

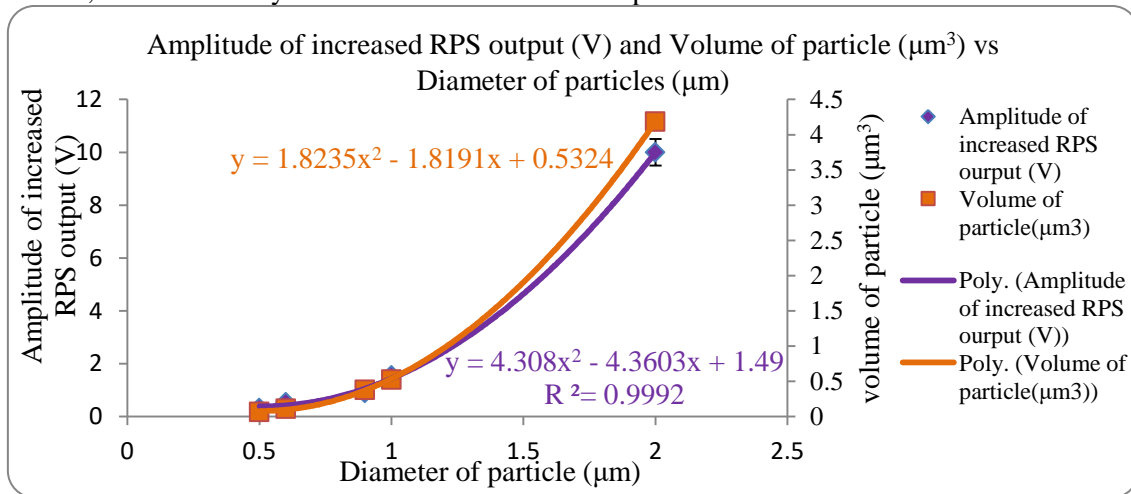


**Figure 3.** Standard curve for relationship between amplitude of RPS output voltage (V), volume of particles (μm³) and diameter of particles (μm).

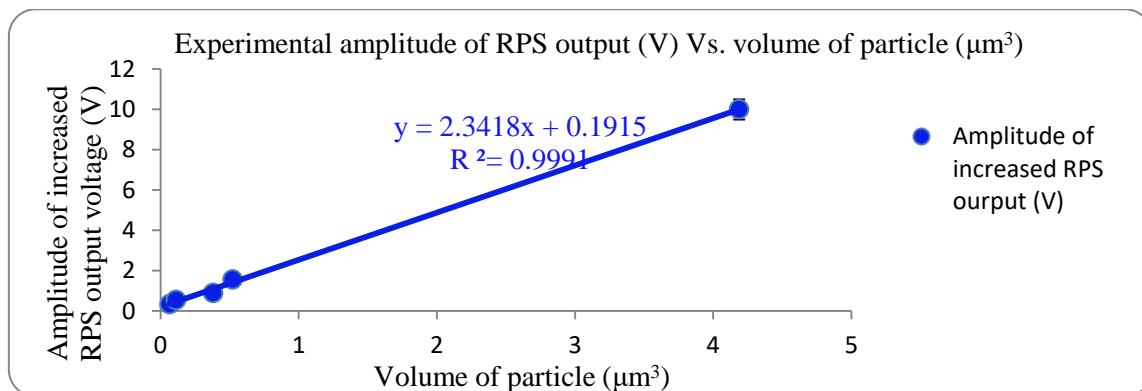


**Figure 4.** The linear relationship graph between amplitude RPS output voltage (V) and volume of particles.

### 3.3. Detecting *Escherichia Coli* and *Enterococci*

Thus as the system ensured reliability, we started to detect the targeted sample bacteria *E.coli* and *Enterococci*. Since the *E.coli* bacteria are non-conductible particles, they become resistors in the electrolyte solution and especially significant when they passed in the detection zone. The voltage is increased at the sensing electrodes as well as the resistance increased in the detection zone. According to the development structure of main channel design and especially the sensing gate area, finally the label free *E.coli* were detected and represented RPS output signals which were shown in Figure 5.

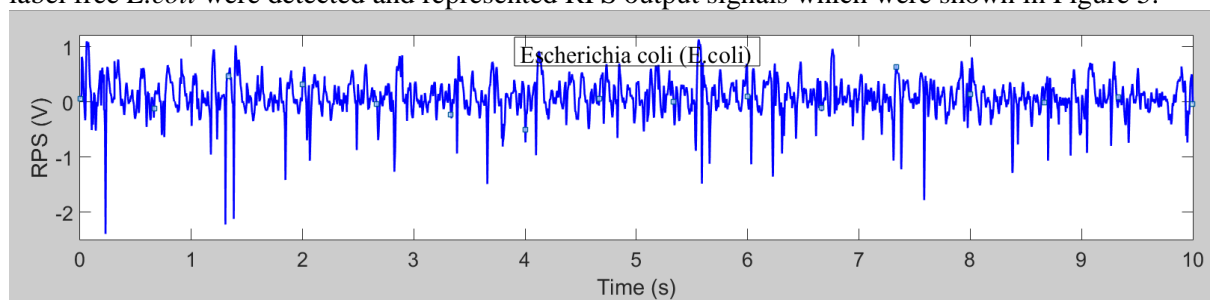


**Figure 5.** The amplitudes of RPS output voltage of *Escherichia coli* in 10sec.

The peak pulse represents the amplitude of increased output voltage when the bacteria passed into the detecting zone. Similarly label-free *Enterococci* were detected by the same above detection protocols and results output signals were received as Figure 6.

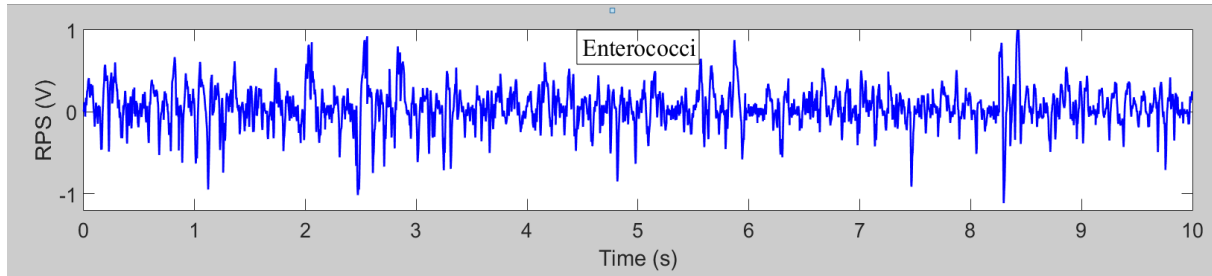


**Figure 6.** The amplitudes of RPS output voltage of *Enterococci* in 10sec.

### 3.4. Double checking the results

The results were double checked with the calculation from theoretical point of view. As indicated by equation (5), the change of resistance is directly proportional to the volume of sample while the inversely correlated to the length and the area of the detection zone. The theoretically calculations of  $\Delta V_{output}$  with equations (1) and (5) by providing the dimension of samples were compared to the experimental result of RPS amplitude as in the following table 1. In addition to, the standard amplitude equation (6) of RPS signal output provides the estimated volume of detected sample and vice-versa.

**Table 1.** The comparison between theoretical and experimental results of MRPS detection system.

Name of sample	Diameter of sample (d) ( $\mu\text{m}$ )	Length of sample (l) ( $\mu\text{m}$ )	Volume of sample (v) ( $\mu\text{m}^3$ )	Theoretical RPS amplitude ( $ \Delta V_{output} $ ) (V)	Experimental RPS amplitude ( $ \Delta V_{output} $ ) (V)	standard curve RPS amplitude ( $ \Delta V_{output} $ ) (V)
<i>E.coli</i>	0.5	1	0.1963	0.46	0.58	0.65
	0.78	2	0.9557	2.23	2.44	2.42
<i>Enterococci</i>	0.45	1	0.159	0.37	0.43	0.56
	0.65	1.5	0.4977	1.167	1.2	1.35

## 4. Conclusion

Compared with the existing problems of heavy equipment, complicated operation, large energy consumption and long-time using, the microfluidic chip based detection system which is proposed in this paper has a good prospect. The detection system uses the microfluidic chip as the detection platform, so that the entire detection process does not require artificial operation, without the need for complex processing before the test. The entire detection process was automatically completed. Utilizing label free bacteria obviated the need for tagging and thus avoids perturbing the biological system. For practical ballast water analysis, a new method has been developed for simple monitoring of bacteriological quality of water. This method is able to provide rapid results, can be easily performed by an analyst with little or no microbiological training. The reliable are and accurate for enumeration of harmful microorganisms. They do not require standard laboratory equipment. The applicability of a Coulter counter based method can be utilised for ballast water quality monitoring involving the enumeration and identification of microorganisms.

## 5. Acknowledgments

This research is supported by National Natural Science Foundation of China (51779027, 51479020 and 51309042), National Key Research and Development Program of China (2017YFC1404603, 2017YFC1404606), Liaoning Provincial Natural Science Foundation of China (2014025017), the Fundamental Research Funds for the Central Universities (3132017076, 3132016325), the Applied

Basic Research Programs of Ministry of Transport of China (2014329225140), and the Basic Research Program of Jiangsu Province (BK20150274).

## 6. References

- [1] Gollasch S, Minchin D and David M 2015 The transfer of harmful aquatic organisms and pathogens with ballast water and their impacts *In Global Maritime Transport and Ballast Water Management* 35-58
- [2] Nghiem LT, Soliman T, Yeo DC, Tan HT, Evans TA, Mumford JD, Keller RP, Baker RH, Corlett RT and Carrasco LR 2013 Economic and environmental impacts of harmful non-indigenous species in Southeast Asia *PLoS One* **8** e71255
- [3] Verna DE and Harris BP 2016 Review of ballast water management policy and associated implications for Alaska *MarPolicy* **70** 13-21
- [4] <https://maritimecyprus.com/2017/07/11/highlights-of-imo-marine-environmentprotection-committee-mepc-71/> (accessed 7 July, 2017)
- [5] David M, Gollasch S and Leppäkoski E 2013 Risk assessment for exemptions from ballast water management—the Baltic Sea case study *Mar pollut bull* **75**, 205-17
- [6] Van Slooten C, Wijers T, Buma AG and Peperzak L 2015 Development and testing of a rapid, sensitive ATP assay to detect living organisms in ballast water *J appl phycol* **27** 2299-312
- [7] Welschmeyer N and Kuo J 2016 Analysis of Adenosine Triphosphate (ATP) as a rapid, quantitative compliance test for ships' ballast water (Final Report) *Broad Agency Announcement (BAA) # HSCG32-13-R-R00016*
- [8] Schillak L 2014 Effective new technologies for the assessment of compliance with the ballast water management convention: final report *BSH Report* Report number: 0014-00007/RO
- [9] MacIntyre HL and Cullen JJ 2016 Classification of phytoplankton cells as live or dead using the vital stains fluorescein diacetate and 5-chloromethylfluorescein diacetate *J phycol* **52** 572-89
- [10] Akram AC, Noman S, Moniri-Javid R, Gizicki JP, Reed EA, Singh SB, Basu AS, Banno F, Fujimoto M and Ram JL 2015 Development of an automated ballast water treatment verification system utilizing fluorescein diacetate hydrolysis as a measure of treatment efficacy *Water res.* **70** 404-13
- [11] Nakata A, Fushida S, Matsuda M and Fukuyo Y 2014 Development of New Method for Estimating Number of Viable Organisms in Ballast Water *T Engineer* **49** 512-17
- [12] Gollasch S and David M 2012 On board tests of the organism detection tools BallastCAM, FluidImaging, USA, Hach-PAM-fluorometer, USA, and Walz-Water-PAM-fluorometer. Results and findings *The Interreg IVB North Sea Ballast Water Opportunity project*
- [13] Olsen RO, Hoffmann F, Hess-Erga OK, Larsen A, Thuestad G and Hoell IA 2016 Ultraviolet radiation as a ballast water treatment strategy: Inactivation of phytoplankton measured with flow cytometry *Mar pollut bull* **103**, 270-275
- [14] Bakalar G and Tomas V 2016 Possibility of using flow cytometry in the treated ballast water quality detection *Pomorski zbornik* **51** 43-55
- [15] Aridgides LJ, Doblin MA, Berke T, Dobbs FC, Matson DO and Drake LA 2004 Multiplex PCR allows simultaneous detection of pathogens in ships' ballast water *Mar pollut bull* **48** 1096-101
- [16] Fykse EM, Nilsen T, Nielsen AD, Tryland I, Delacroix S and Blatny JM 2012 Real-time PCR and NASBA for rapid and sensitive detection of *Vibrio cholerae* in ballast water *Mar pollut bull* **64** 200-6
- [17] Zheng Y, Nguyen J, Wei Y and Sun Y 2013 Recent advances in microfluidic techniques for single-cell biophysical characterization *Lab Chip* **13** 2464- 83
- [18] Ma X and Huo YX 2016 The application of microfluidic-based technologies in the cycle of metabolic engineering *Synthetic and Systems Biotechnology* **1** 137-42
- [19] Cho YH, Yamamoto T, Sakai Y, Fujii T and Kim B 2006 Development of microfluidic device for electrical/physical characterization of single cell *J Microelectromech S* **15** 287-95
- [20] Guan X, Zhang HJ, Bi YN, Zhang L and Hao DL 2010 Rapid detection of pathogens using antibody-coated microbeads with bioluminescence in microfluidic chips *Biomed microdevices* **12** 683-91



- [21] Fang C et al 2010 Integrated microfluidic and imaging platform for a kinase activity radioassay to analyze minute patient cancer samples *Cancer res* **70** 8299-308
- [22] Sia SK and Whitesides GM 2003 Microfluidic devices fabricated in poly (dimethylsiloxane) for biological studies *Electrophoresis* **24** 3563-76
- [23] Park S, Zhang Y, Lin S, Wang TH and Yang S 2011 Advances in microfluidic PCR for point-of-care infectious disease diagnostics *Biotechnol adv* **29** 830-39
- [24] Joachimsthal EL, Ivanov V, Tay SL and Tay JH 2004 Bacteriological examination of ballast water in Singapore Harbour by flow cytometry with FISH *Mar pollut bull* **49** 334-43
- [25] Meagher RJ and Wu M 2016 Microfluidic Approaches to Fluorescence In Situ Hybridization (FISH) for Detecting RNA Targets in Single Cells *SpringerInternational Publishing, InMicrofluidic Methods for Molecular Biology* 95-112
- [26] Walter A, März A, Schumacher W, Rösch P and Popp J 2011 Towards a fast, high specific and reliable discrimination of bacteria on strain level by means of SERS in a microfluidic device *Lab Chip* **11** 1013-21
- [27] Knauer M, Ivleva NP, Niessner R and Haisch C 2012 A flow-through microarray cell for the online SERS detection of antibody-captured E. coli bacteria *Anal bioanal chem* **402** 2663-67
- [28] Saleh OA 2003 A novel resistive pulse sensor for biological measurements. Doctoral dissertation Princeton University
- [29] DeBlois RW and Bean CP 1970 Counting and sizing of submicron particles by the resistive pulse technique *Review of Scientific Instruments* **41** 909-916
- [30] Kasianowicz JJ, Brandin E, Branton D and Deamer DW 1996 Characterization of individual polynucleotide molecules using a membrane channel *P Natl A Sci* **93** 13770-13773
- [31] Bryan AK, Engler A, Gulati A and Manalis SR 2012 Continuous and longterm volume measurements with a commercial Coulter counter *Plos one* **7** e29866
- [32] Blundell EL, Mayne LJ, Billinge ER and Platt M 2015 Emergence of tunable resistive pulse sensing as a biosensor *Anal Methods-UK* **7** 7055-66
- [33] Yang L and Yamamoto T 2016 Quantification of virus particles using nanopore-based resistive-pulse sensing techniques *Front microbiol*
- [34] Cheung KC, Di Berardino M, Schade- Kampmann G, Hebeisen M, Pierzchalski A, Bocsi J, Mittag A and Tárnok A 2010 Microfluidic impedance-based flow cytometry *Cytom Part A* **77**, 648-66
- [35] Wang J, ZhaoJ, Wang Y, Wang W, Gao Y, Xu R and Zhao W 2016 A new microfluidic device for classification of microalgae cells based on simultaneous analysis of chlorophyll fluorescence, side light scattering, resistance pulse sensing *Micromachines* **7** 198
- [36] Kozak D, Anderson W, Vogel R and Trau M 2011 Advances in resistive pulse sensors: devices bridging the void between molecular and microscopic detection *Nano Today* **6** 531-45
- [37] Wang J, Song Y, Maw MM, Song Y, Pan X, Sun Y and Li D 2015 Detection of size spectrum of microalgae cells in an integrated underwater microfluidic device *J Exp Mar Biol Ecol* **473** 129-37
- [38] Maw MM, Wang J, Li F, Jiang J, Song Y and Pan X 2015 Novel electrokinetic microfluidic detector for evaluating effectiveness of microalgae disinfection in ship ballast water *Int j mol sci* **16** 25560-75
- [39] Golibersuch DC 1973 Observation of aspherical particle rotation in Poiseuille flow via the resistance pulse technique: I. Application to human erythrocytes *Biophysical journal* **13** 265-80
- [40] Maw MM, Pan X, Peng Z, Wang Y, Zhao L, Dai B and Wang J 2018 A changeable lab-on-a-chip detector for marine nonindigenous microorganisms in ship's ballast water. *Micromachines* **9** 20
- [41] Russakoff G 1970 A derivation of the macroscopic Maxwell equations. *Am J Phys* **38** 1188-95
- [42] Raviart PA and Sonnendrücker E 1995 Approximate models for the Maxwell equations *J comput appl math* **63** 69- 81